JOURNAL OF GEOPHYSICAL RESEARCH, VOL. 108, NO. D4, 4140, doi:10.1029/2002JD002887, 2003

Comparison between active sensor and radiosonde cloud boundaries over the ARM Southern Great Plains site

Catherine M. Naud and Jan-Peter Muller
Geomatic Engineering, University College, London, UK

Eugene E. Clothiaux
Pennsylvania State University, University Park, Pennsylvania, USA

Received 27 August 2002; revised 4 December 2002; accepted 16 December 2002; published 27 February 2003.

[1] In order to test the strengths and limitations of cloud boundary retrievals from radiosonde profiles, 4 years of radar, lidar, and ceilometer data collected at the Atmospheric Radiation Measurements Southern Great Plains site from November 1996 through October 2000 are used to assess the retrievals of *Wang and Rossow* [1995] and *Chernykh and Eskridge* [1996]. The lidar and ceilometer data yield lowest-level cloud base heights that are, on average, within approximately 125 m of each other when both systems detect a cloud. These quantities are used to assess the accuracy of coincident cloud base heights obtained from radar and the two radiosonde-based methods applied to 200 m resolution profiles obtained at the same site. The lidar/ceilometer and radar cloud base heights agree by 0.156 ± 0.423 km for 85.27% of the observations, while the agreement between the lidar/ceilometer and radiosonde-derived heights is at best -0.044 ± 0.559 km for 74.60% of all cases. Agreement between radar- and radiosonde-derived cloud boundaries is better for cloud base height than for cloud top height, being at best 0.018 ± 0.641 km for 70.91% of the cloud base heights and 0.348 ± 0.729 km for 68.27% of the cloud top heights. The disagreements between radar- and radiosonde-derived boundaries are mainly caused by broken cloud situations when it is difficult to verify that drifting radiosondes and fixed active sensors are observing the same clouds. In the case of the radar the presence of clutter (e.g., vegetal particles or insects) can affect the measurements from the surface up to approximately 3–5 km, preventing comparisons with radiosonde-derived boundaries. Overall, *Wang and Rossow* [1995] tend to classify moist layers that are not clouds as clouds and both radiosonde techniques report high cloud top heights that are higher than the corresponding heights from radar. *INDEX TERMS:* 0320 Atmospheric Composition and Structure: Cloud physics and chemistry; 0394 Atmospheric Composition and Structure: Instruments and techniques; 1610 Global Change: Atmosphere (0315, 0325); 1640 Global Change: Remote sensing; 1694 Global Change: Instruments and techniques

Citation: Naud, C. M., J.-P. Muller, and E. E. Clothiaux, Comparison between active sensor and radiosonde cloud boundaries over the ARM Southern Great Plains site, *J. Geophys. Res.*, *108*(D4), 4140, doi:10.1029/2002JD002887, 2003.

1. Introduction

[2] The overall impact of clouds on the energy budget of the Earth is difficult to estimate as it involves two opposite effects depending on cloud type. Low highly reflective clouds tend to cool the surface, whereas high semitransparent clouds tend to warm it. To improve the predictive capabilities of large-scale models, one needs accurate observations of both global cloud amount and the vertical distributions of clouds. Satellite measurements have the advantage of providing global cloud coverage, but retrieving accurate cloud top heights from satellite has yet to be demonstrated. To validate satellite-derived cloud boundaries, ground- and airborne-based instruments are commonly used [e.g., *Smith and Platt*, 1978; *Baum et al.*, 1995; *Ou et al.*, 1998; *Marchand et al.*, 2001; *Trishchenko et al.*, 2001]. The usefulness of ground-based active sensors, such as radars, laser ceilometers, and lidars, for this purpose has been extensively demonstrated [e.g., *Mace et al.*, 1998; *Clothiaux et al.*, 2000; *Dong et al.*, 2000], but their global coverage is sparse with results restricted to a few locations. Their greatest advantage is their accuracy, continuous temporal sampling, and large vertical coverage.

[3] One drawback to ground-based remote sensors occurs in conditions when the lasers cannot penetrate to the top of the highest-cloud layer. Lack of radar sensitivity to the smallest-cloud particles (i.e., approximately 1–10 μm in radius) prevents unambiguous determination of the absence of small particles in these regions. Consequently, the failure of radar to detect the tops of the highest clouds, which is a

0148-0227/03/2002JD002887

distinct possibility, leads to underestimation of cloud top height for these cases. In fact, for all locations where small cloud particles are sampled by the radar, but not the lidar/ceilometer pair, the active sensor instruments may fail to detect them, especially as the distance between the radar and these small particles increases.

[4] Another type of instrument that covers a large vertical extent is a radiosonde. Radiosondes also have the advantage of being widely used, available at a large number of locations (although underrepresented over oceans) and used for many decades. They represent an excellent means for validating satellite measurements of cloud top height if one can retrieve cloud boundaries from temperature and humidity profiles. To date, they have been mainly used to validate satellite cloud top wind retrievals [e.g., *Schmetz et al.*, 1993; *Menzel*, 2001]. Another important application of radiosondes is the development of cloud climatology. Using a global data set of radiosondes collected over 20 years, *Wang et al.* [2000] studied cloud base height (CBH), cloud top height (CTH), and cloud layer thickness occurrences and estimated their average values and variations for different climatic regions. Similarly, *Chernykh et al.* [2001] selected 967 stations that were distributed all over the globe and studied 795 time series over a period of 34 years from 1964 to 1998. They found that CBHs have decreased by about 150 m over these 34 years, while CTHs have increased by 450 m.

[5] In recent years, there has been renewed interest in radiosonde data for cloud detection and characterization, and several methods have been presented [*Poore et al.*, 1995; *Wang and Rossow*, 1995; *Chernykh and Eskridge*, 1996; *Wang et al.*, 1999, 2000; *Chernykh et al.*, 2001]. So far, three different approaches have been used: (1) cloud layers are detected using a threshold on relative humidity at mandatory and significant levels [e.g., *Poore et al.*, 1995; *Wang and Rossow*, 1995; *Wang et al.*, 1999, 2000]; (2) cloud layers are detected based on a diagram that relates temperature and relative humidity at all levels [e.g., *Arabey*, 1975 and references therein]; and (3) cloud layers are detected from variations (i.e., inflexion points) in the temperature and relative humidity profiles and a diagram similar to that used by Arabey [e.g., *Chernykh and Eskridge*, 1996; *Chernykh et al.*, 2001].

[6] *Poore et al.* [1995], *Wang and Rossow* [1995] (hereinafter referred to as WR95), and *Wang et al.* [2000] transformed relative humidity measurements with respect to ice for all levels below 0°C and applied a threshold of 84% on the relative humidity to detect moist layers. They subsequently used a second threshold of 87% to characterize a moist layer as a cloud layer. However, their two thresholds are the same at all altitudes. *Slingo* [1980] defined different thresholds for low-, mid- and high-level clouds for a numerical model cloud parameterization. Following this work, *Han and Ellingson* [2000] used laser ceilometer data at the US Department of Energy Atmospheric Radiation Measurements (ARM) Program Southern Great Plains (SGP) site in broken cloud situations to verify that there is a decrease in relative humidity at cloud base as the CBH increases, at least up to heights of 2.5 km. *Chernykh* [1999] found this same relationship between relative humidity and CBH for all cloud layers.

[7] *Chernykh and Eskridge* [1996] (hereinafter referred to as CE96) have proposed an alternative technique to detect cloud layers; the second-order derivatives with respect to the height of the temperature and relative humidity are positive and negative, respectively, within cloud layers and the boundaries are defined where at least one of the two second derivatives is zero. They compared their retrievals with ground observations and found that 90% of the cases studied were consistent. However, ground observers can only give information on cloud base. The CE96 technique has also been compared with other instruments during SHEBA [*Curry et al.*, 2000], but this validation exercise was conducted only over a month [*Chernykh and Alduchov*, 2000].

[8] The objective of this study is to test how active sensor and radiosonde retrieval of cloud boundaries compare using collocated data over a long time period. The goal is to understand the strengths and limitations of these two distinctly different methods for retrieving cloud boundaries. We compare cloud base and top heights retrieved with radiosonde profiles collected at the ARM SGP site from November 1996 through October 2000 with those simultaneously retrieved from a collocated radar and lidar. (These data sets are described in section 2.) We use the WR95 and CE96 techniques (section 3) to retrieve CBH of the lowest cloud and CTH of the highest cloud using the dry temperature, dew-point temperature, pressure, and relative humidity profiles from radiosondes. These retrievals are then compared (section 4) to the cloud base and top heights obtained from the radar and lidar measurements using the processing chain developed by *Clothiaux et al.* [2000] and radiosonde detection and retrieval accuracies are assessed.

2. ARM SGP Radiosonde and Active Remote Sensor Data

[9] Temperature, relative humidity, and pressure profiles measured by radiosondes are primary products, while level heights are a derived product. The radiosonde data collected at the ARM SGP site are measured every 2 s, which gives a measurement on average every 10 m. According to instrument specifications, the precision for the temperature and relative humidity measurements is 0.1°C and 1%, respectively. Considering an adiabatic lapse rate for temperature of 6°C/km, the temperature would change by 0.06°C in 10 m, which is too small to be reliably detected in analysis of the radiosonde measurements. Inspecting the NCEP-NCAR reanalysis display facility (available as: http://www.cdc.noaa.gov/cdc/data.ncep.reanalysis.derived.html#pressure), we found a gradient of approximately 6%/km for the long term yearly average relative humidity variation between 1000 and 400 mb, which implies a change of 0.06% every 10 m and is again smaller than the precision of the radiosonde measurement.

[10] For both the temperature and relative humidity, measurements every 100 m would be sufficient to ensure that errors in gradients computed from the measurements are far less than the expected rates of change in the measurements. Measurements every 200 m are a better compromise, with 500-m measurements most likely leading to the smallest errors in the computed gradients. However, as the measurement spacing goes up, the resolution of the cloud boundary estimates goes down. *Chernykh and Aldu-*

chov [2000] have shown that the best results in cloud boundary retrievals were obtained for spacings between consecutive levels of 100 m in the boundary layer with a minimum cloud thickness of 50 and 300–600 m in the free troposphere. However, methods such as WR95 that use thresholds on relative humidity to derive cloud boundaries perform better with smaller spacings between levels. Eskridge and Alduchov (private communication, 2001) recommended using at least a 200-m spacing between measurements, so we adopted the method used by CE96, which is to reduce the measurement frequency by selecting only the significant and mandatory levels [*Office of the Federal Coordinator for Meteorology*, 1997] while adding levels between existing levels that are separated by more than 200 m. For the SGP site radiosondes, we generally retained about 50 measurement levels per sounding with this approach. For the period from November 1996 through October 2000, there were a total of 3334 soundings that were utilized in this study.

[11] The 35-GHz MilliMeter wavelength Cloud Radar (MMCR) data have been processed using the algorithm developed by *Clothiaux et al.* [2000]. The product used here is the "Quality Checked Reflectivity Clutter Flag," which gives, as a function of time (every 10 s) and altitude (every 45 m and adjusted to be above mean sea level (MSL)), the following values: clear, 0; cloud, 1; mixed cloud and clutter, 2; clutter with only nonhydrometeor objects detected, 3; and no data, 10. For each day within the period covered by both data sets, we eliminated all those data records when there were no radar, lidar/ceilometer or radiosonde data available. For each radiosonde sounding, we checked the time that elapsed between its launch and it reaching an altitude of 12 km, which is approximately the height of the tropopause in a US standard atmosphere. On average, this time was about 40–60 min. We then examined the radar profiles over this time period, assigning a cloud flag to any altitude where at least one cloud or cloud-clutter flag occurred within the time period. We then assigned CBH to the cloud flag with the lowest altitude and CTH to the cloud flag with the highest altitude. We hereafter refer to these two heights per sounding as the radar minimum CBH and the radar maximum CTH. This method tends to underestimate CBH and overestimate both CTH and layer thickness within the period, but it allows for the detection of clouds in broken cloud situations.

[12] For each time period, we also computed the median values of the cloud base and top heights that were retrieved on a profile-by-profile basis. We hereafter refer to these two heights per time period as the radar median cloud base and top heights. When extracting the median values for cloud base and top height for each time period, we also tallied the percentage of radar profiles containing at least one cloud flag to provide a measure of the radar-derived cloud fraction for the time period.

[13] Among the various products available in the processed radar data product, we also used the Laser Cloud Base Best Estimate (LaserCBBE) that is derived from a combination of micropulse lidar and Belfort laser ceilometer CBH estimates. The ceilometer data are generally used in the lower troposphere for the best estimate of CBH, as its spatial resolution is higher than for the lidar, while the lidar CBH estimates, which are derived with two distinct algorithms, are taken as the best estimates of CBH above approximately 5 km of altitude [*Clothiaux et al.*, 2000]. Similar to the radar, the LaserCBBE parameter is collected over the time it takes for the radiosonde to reach 12 km of altitude. We compute the median LaserCBBE height, referenced above MSL, and cloud fraction for each sounding, just as we did in the analysis of the radar data. We also compute the median LaserCBBE over a time period covering ±3 hours centered on the time of launch, which we refer to as the 3 hours LaserCBBE, as well as the corresponding cloud fraction and percent occurrence of precipitation. Knowledge of precipitating periods is important as precipitation affects the quality of the lidar and ceilometer, as well as the radar, CBH retrievals.

[14] The lidar and ceilometer data yield lowest-level CBHs that are, on average, within approximately 125 m of each other when both systems detect a cloud, even though the two systems implement two different CBH retrieval algorithms [*Clothiaux et al.*, 1998]. Consequently, for non-precipitating cloud conditions we expect the retrieved CBHs to be accurate to within approximately 125 m. Identification of CBH in regions of clouds with substantial subcloud drizzle is difficult with backscatter lidars and ceilometers and CBH retrieval accuracy is degraded in these conditions. Radar performance has been compared with the lidar and ceilometer in the work of *Clothiaux et al.* [2000]. They show that the radar fails to detect a cloud identified by the lidar/ceilometer pair in only 5.9% of all cases when using all four operational modes of the radar. They found that the clouds most often missed by the radar were either composed of small particles or thin clouds (e.g., thin stratus and cirrus and fair weather cumulus).

3. Cloud Boundary Retrievals Using Radiosonde Data

[15] The WR95 method for analyzing relative humidity profiles is based on the approach of *Poore et al.* [1995]. The profiles are sampled at least every 200 m following the method described in the previous section. WR95 convert relative humidity measurements into relative humidity with respect to ice when the temperature drops below 0°C in the sounding, and they subsequently examine the relative humidity profile in four steps, starting from the surface level upwards: (1) the first level above the surface both with a relative humidity of at least 84% and with an increase in relative humidity, from the level below, of at least 3% is taken to be the beginning of the lowest-altitude moist layer; (2) contiguous levels above the base of the moist layer with relative humidity of at least 84% are part of the moist layer; (3) the top of the moist layer is reached when the relative humidity decreases by more than 3% below the 84% threshold; and (4) the moist layer is classified as a cloud if the relative humidity exceeds 87% somewhere within it. Starting from the level above a moist layer, this four-step process is repeated to the top of the profile.

[16] Cloud layers starting at the ground have their bases set to 500 m Above Ground Level (AGL) and are discarded if their tops are less than 500 m AGL. WR95 chose 500 m as the lowest possible CBH after analyzing retrievals from ground observers in situations when a moist layer is detected at ground level but clouds are observed higher.

These conditions are associated with fog, drizzle, or rain below cloud or when the surface is very humid. Single-level cloudy layers have their base height set halfway to the level below and their top height set halfway to the next level above. The minimum (84%) and maximum (87%) thresholds were derived from measured relative humidity with VIZ-type radiosondes at CBHs estimated from surface observations. Note that *Wang et al.* [1999] have used thresholds of 90 and 93% to overcome the problem of false positive cloud detections near the surface. We use here the 84 and 87% thresholds and test the 90 and 93% thresholds when appropriate.

[17] We applied the four steps of WR95 to the processed SGP radiosonde profiles after transforming the relative humidity measurements with respect to ice following the relation proposed by *Alduchov and Eskridge* [1996]. Cloud layers with top heights below 827 m MSL (i.e., 512 m AGL at SGP) were discarded, while cloud layers with base heights less than 827 m MSL and top heights above 827 m MSL were kept. Even though this 500 m AGL threshold was derived for a particular location, we used it here since no weather information was available that allowed us to derive a new value.

[18] CE96 apply spline fits to the processed radiosonde profiles to compute the second-order derivatives of temperature and relative humidity with height. Layers are classified as moist when the second-order derivative of the temperature in them is positive and the second-order derivative of their relative humidity is negative. Because cloud boundaries can be identified when a cloud is not fully formed, a cloud has already dissipated, or a cloud can be found in a neighboring region (i.e., in broken cloud conditions), CE96 use a diagram developed by *Arabey* [1975] that predicts the cloud amount within a layer based on an empirical relationship between the dew-point depression and the temperature in this layer. The diagram gives four ranges of cloud amount: 80–100, 60–80, 20–60, and 0–20% (clear sky). For this study, the approach of CE96 with the 80–100% cloud amount will be used as the criterion for cloud presence, which we refer to as the CE9680 approach. For some occasions, we test for cloud occurrence using the 60–100 and 20–100% cloud amounts, referring to these tests as CE9660 and CE9620, respectively. *Chernykh and Alduchov* [2000] also impose a minimum vertical extent on each cloudy layer. We did not incorporate this additional condition in the current study as we found that single-level clouds detected with CE9680 are within 2 km of LaserCBBE and Radar Cloud Top Height (RadarCTH) in about 80 and 70% of all cases when detected.

4. Comparison of Active Remote Sensor and Radiosonde-Retrieved Cloud Base and Top Heights

[19] In the comparison of active remote sensor and radiosonde-retrieved cloud base and top heights, we actually perform seven different comparisons. First, we compare lidar/ceilometer (i.e., laser) median LaserCBBE with median radar cloud base height (RadarCBH) in order to assess our methods for processing the radar reflectivity clutter flag and to understand the accuracy of the radar retrievals with respect to those from the lasers. We then perform the following six comparisons: (1) Median LaserCBBE versus *Chernykh and Eskridge* [1996] cloud base height (CE9680CBH and CE9660CBH), (2) median LaserCBBE versus *Wang and Rossow* [1995] cloud base height (WR95CBH), (3) median RadarCBH versus *Chernykh and Eskridge* [1996] cloud base height (CE9680CBH and CE9660CBH), (4) median RadarCBH versus *Wang and Rossow* [1995] cloud base height (WR95CBH), (5) RadarCTH versus *Chernykh and Eskridge* [1996] cloud top height (CE9680CTH and CE9660CTH), and (6) median RadarCTH versus *Wang and Rossow* [1995] cloud top height (WR95CTH). The results of these comparisons can be found in Table 1 and Figures 1 and 2.

[20] Since the LaserCBBE and RadarCBH estimates are in fair agreement with each other and produce similar results in comparison with the radiosonde retrievals, we discuss only the comparisons of LaserCBBE with the radiosonde retrievals of CBH, limiting discussion of the radar retrievals to their comparison with radiosonde-derived CTHs. For the CTH comparisons, we have to rely on the accuracy of the radar retrievals, bearing in mind that for CTHs with altitudes less than approximately 5 km there could be problems with clutter contamination of the radar returns and that the radar may have insufficient sensitivity to detect the top of the highest-cloud layer.

[21] For each of the seven comparisons, we compute the number of clear-sky periods identified simultaneously by both retrieval techniques (Table 1, row 4), the number of cloudy-sky periods identified simultaneously by both retrieval techniques (Table 1, row 7), and the number of cloudy-sky periods identified by one instrument and not the other (Table 1, rows 5 and 6). We illustrate the frequencies of occurrence of cloud base and top heights when both retrievals detect a cloud, as well as the frequencies of occurrence of cloud base and top heights when one retrieval indicates cloud and the other does not (Figure 1).

[22] In order to assess the performance of each retrieval technique with respect to the reference, or "truth," measurements (i.e., LaserCBBE and RadarCTH), we used the following quantities to characterize cloud detection accuracy. (1) Detection efficiency: the ratio of the number of total positive detections (i.e., both instruments detect a cloud) to the sum of total positive detections and false positive detections (i.e., the reference instrument does not detect a cloud whereas the other instrument does). (2) Detection quality: the ratio of the number of total positive detections to the sum of total positive detections, false positive detections, and false negative detections (i.e., the reference instrument detects a cloud whereas the other instrument does not). The values for these two quantities are also provided in Table 1, row 8. Finally, for those time periods (i.e., soundings) when both retrieval techniques indicate cloud we produce scatterplots of the height differences between the two retrievals (Figure 2) and the accuracy of each method with respect to the reference measurement is calculated and reported in Table 1 (rows 7, 9, 10, and 11). We now discuss in more detail the salient results illustrated in the table and figures.

4.1. LaserCBBE Versus RadarCBH

[23] Of the 131 CBHs in RadarCBH not contained in LaserCBBE (Table 1, column 3), 106 cases have radar

Table 1. Summary of 13 Comparisons Between Measurements A (Row 1) and B (Row 2)[a]

Rows	Sample	i	ii	iii	iv	v	vi	vii	viii	ix	x	xi	xii	xiii
1	A	LaserCBBE	LaserCBBE	LaserCBBE	LaserCBBE	LaserCBBE	RadarCBH	RadarCBH	RadarCTH	RadarCTH	RadarCTH	RadarCTH	CE96HYCBH	CE9680CTH
2	B	RadarCBH	CE9680CBH	CE9660CBH	CE96HYCBH	WR95CBH	CE9680CBH	WR95CBH	CE9680CTH	CE9660CTH	CE96HYCTH	WR95CTH	WR95CBH	WR95CTH
3	Samples total	3334	3334	3334	3334	3334	3334	3334	3334	3334	3334	3334	3334	3334
4	Samples clear: A and B	898 (26.93%)	949 (28.46%)	671 (20.13%)	671 (20.13%)	871 (26.12%)	995 (29.84%)	903 (27.08%)	995 (29.84%)	669 (20.07%)	669 (20.07%)	903 (27.08%)	835 (25.05%)	1207 (36.20%)
5	Samples cloudy: A not B	219 (6.57%)	669 (20.07%)	190 (5.70%)	190 (5.70%)	446 (13.38%)	623 (18.69%)	414 (12.42%)	623 (18.69%)	192 (5.76%)	192 (5.76%)	414 (12.42%)	483 (14.49%)	111 (3.33%)
6	Samples cloudy: B not A	131 (3.93%)	80 (2.4%)	358 (10.73%)	358 (10.73%)	159 (4.77%)	122 (3.66%)	216 (6.48%)	122 (3.66%)	448 (13.44%)	448 (13.44%)	216 (6.48%)	29 (0.87%)	414 (12.42%)
7	Samples cloudy: A and B	2086 (62.57%) 0.018 ± 1.559 km 0.91	1636 (49.07%) -0.475 ± 2.303 km 0.83	2115 (63.44%) 0.493 ± 2.517 km 0.80	2115 (63.44%) -0.054 ± 2.454 km 0.81	1858 (55.73%) 0.698 ± 2.240 km 0.78	1594 (47.81%) -0.540 ± 2.483 km 0.80	1801 (54.02%) 0.651 ± 2.513 km 0.73	1594 (47.81%) -0.852 ± 3.114 km 0.78	2025 (60.73%) -2.421 ± 3.678 km 0.67	2025 (60.73%) -2.407 ± 3.688 km 0.67	1801 (54.02%) -0.478 ± 2.944 km 0.74	1987 (59.60%) 0.599 ± 2.156 km 0.80	1602 (48.05%) 0.131 ± 2.430 km 0.87
8	Detection efficiency & quality	94.09% 85.63%	95.34% 68.60%	85.52% 79.42%	85.52% 79.42%	92.12% 75.44%	92.89% 68.15%	89.29% 74.09%	92.89% 68.15%	81.88% 75.99%	81.88% 75.99%	89.29% 74.09%	98.56% 79.51%	79.46% 75.32%
9	$\|A-B\| \leq$ 2 km	1945 (93.24%) 0.156 ± 0.423 km 0.99	1381 (84.41%) -0.191 ± 0.586 km 0.99	1786 (84.45%) 0.088 ± 0.579 km 0.99	1816 (85.86%) -0.044 ± 0.559 km 0.99	1578 (84.93%) 0.192 ± 0.564 km 0.99	1273 (79.86%) -0.310 ± 0.656 km 0.99	1461 (81.12%) 0.018 ± 0.641 km 0.98	1202 (75.41%) -0.349 ± 0.745 km 0.99	1207 (59.60%) -0.562 ± 0.737 km 0.99	1207 (59.60%) -0.539 ± 0.757 km 0.99	1373 (76.24%) -0.348 ± 0.729 km 0.98	1781 (89.63%) 0.177 ± 0.426 km 0.99	1357 (84.71%) -0.081 ± 0.484 km 0.99
10	$A-B >$ 2 km	55 (2.64%)	75 (4.59%)	253 (11.96%)	164 (7.76%)	230 (12.38%)	96 (6.02%)	259 (14.38%)	107 (6.71%)	59 (2.92%)	59 (2.92%)	159 (8.83%)	167 (8.41%)	131 (8.18%)
11	$A-B <$ −2 km	86 (4.12%)	180 (11.0%)	76 (3.59%)	135 (6.38%)	50 (2.69%)	225 (14.12%)	81 (4.50%)	285 (17.88%)	759 (37.48%)	759 (37.48%)	269 (14.93%)	39 (1.96%)	114 (7.12%)

[a]Row 3, total number of compared cases; row 4, total number of cases with A and B clear (with percentage from total); rows 5 and 6, false cloud detections (false negatives: A cloudy and B clear, and false positives: A clear and B cloudy) with corresponding percentage from total; row 7, total number of A and B cloudy (with percentage from total) with average difference, standard deviation, and correlation coefficient; row 8, detection efficiency and quality percentages; row 9, number of cases with difference within 2 km including percentage from total positive, average difference, standard deviation, and correlation coefficient; row 10, number of cases with difference greater than 2 km with percentage from total positive; row 11, number of cases with difference less than −2 km with percentage from total positive.

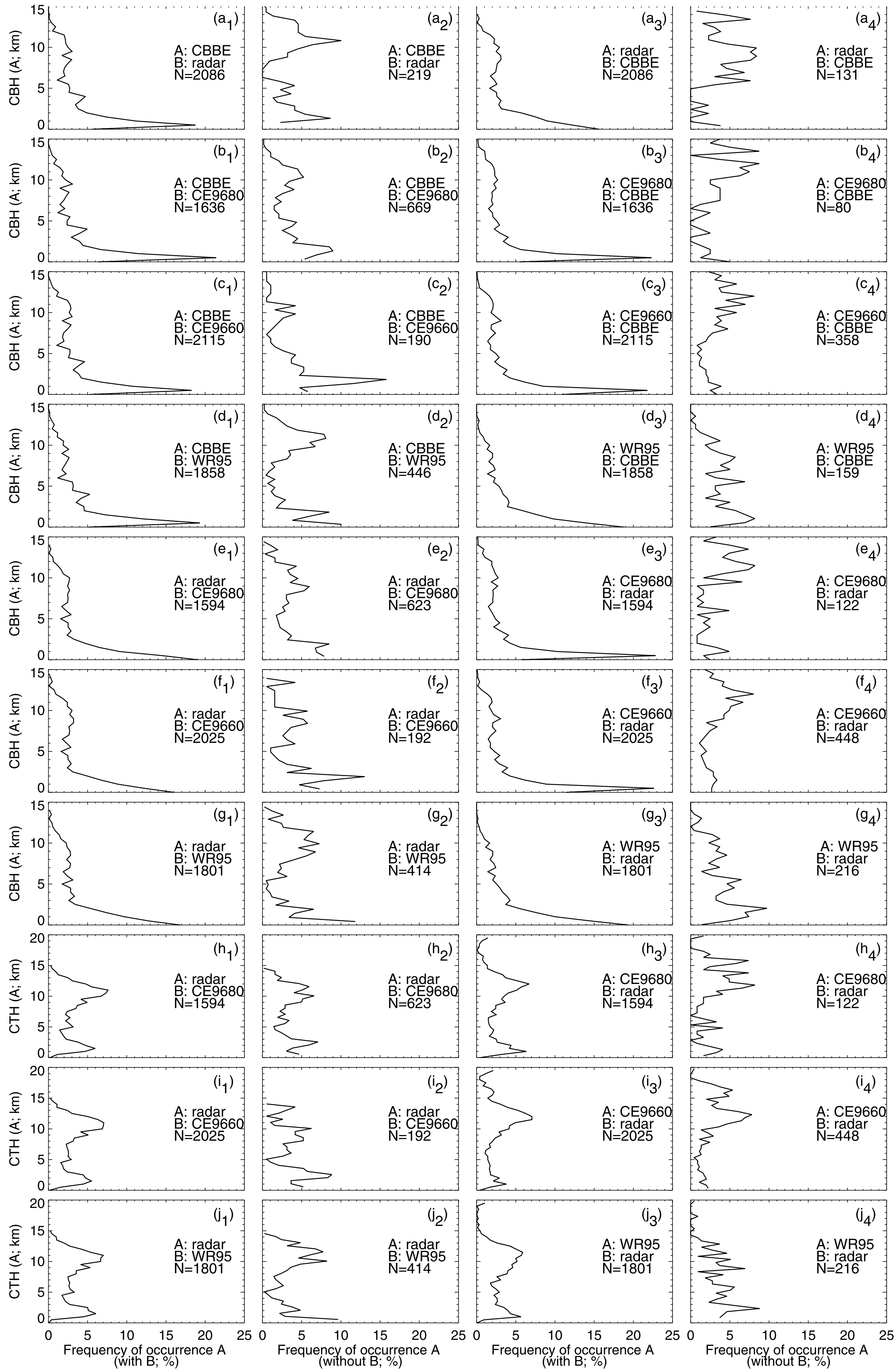
(a1) A: CBBE B: radar N=2086
(a2) A: CBBE B: radar N=219
(a3) A: radar B: CBBE N=2086
(a4) A: radar B: CBBE N=131
(b1) A: CBBE B: CE9680 N=1636
(b2) A: CBBE B: CE9680 N=669
(b3) A: CE9680 B: CBBE N=1636
(b4) A: CE9680 B: CBBE N=80
(c1) A: CBBE B: CE9660 N=2115
(c2) A: CBBE B: CE9660 N=190
(c3) A: CE9660 B: CBBE N=2115
(c4) A: CE9660 B: CBBE N=358
(d1) A: CBBE B: WR95 N=1858
(d2) A: CBBE B: WR95 N=446
(d3) A: WR95 B: CBBE N=1858
(d4) A: WR95 B: CBBE N=159
(e1) A: radar B: CE9680 N=1594
(e2) A: radar B: CE9680 N=623
(e3) A: CE9680 B: radar N=1594
(e4) A: CE9680 B: radar N=122
(f1) A: radar B: CE9660 N=2025
(f2) A: radar B: CE9660 N=192
(f3) A: CE9660 B: radar N=2025
(f4) A: CE9660 B: radar N=448
(g1) A: radar B: WR95 N=1801
(g2) A: radar B: WR95 N=414
(g3) A: WR95 B: radar N=1801
(g4) A: WR95 B: radar N=216
(h1) A: radar B: CE9680 N=1594
(h2) A: radar B: CE9680 N=623
(h3) A: CE9680 B: radar N=1594
(h4) A: CE9680 B: radar N=122
(i1) A: radar B: CE9660 N=2025
(i2) A: radar B: CE9660 N=192
(i3) A: CE9660 B: radar N=2025
(i4) A: CE9660 B: radar N=448
(j1) A: radar B: WR95 N=1801
(j2) A: radar B: WR95 N=414
(j3) A: WR95 B: radar N=1801
(j4) A: WR95 B: radar N=216
CBH (A; km)
CTH (A; km)
Frequency of occurrence A (with B; %)
Frequency of occurrence A (without B; %)

cloud detections for less than 5 min over the observational time period and are most likely erroneous, 5 cases have the precipitation flag turned on over a large portion of the observational period and are for periods when the lidar/ceilometer processing most likely failed, 13 cases are for scattered clouds where the 3 hours LaserCBBE contains a CBH at a similar altitude to RadarCBH and 7 cases have no 3 hours CBBE detections, or, if there are, the clouds detected are lower than for RadarCBH. We suspect that for these last seven cases there may have been problems in the LaserCBBE processing or measurements, such as the lack of lidar data, which limit the vertical range of LaserCBBE to below 5 km AGL. Of the 219 cases in LaserCBBE not contained in RadarCBH, 176 cases have LaserCBBE cloud fractions less than 0.5 (i.e., broken cloud cases that the radar most likely cannot detect), while 9 cases are for LaserCBBE below 5 km and 34 cases are for LaserCBBE above 5 km. For LaserCBBE below 5 km, one case has radar clutter at LaserCBBE, four cases show radar clutter, or a mixture of cloud and clutter, at the LaserCBBE, but either before or after the time of observation, and four cases have so-called "bad" radar data, i.e., there were problems with the radar data processing routine with the result that while no measurements seem to have been taken during the case study period the processed data nonetheless indicate a "clear" situation. For LaserCBBE above 5 km, apart from four cases that contain bad radar data, the problem seems to be an insufficient sensitivity of the radar to detect all of the cloud elements in high thin cirrus detected by the lidar. The radar detection efficiency with respect to the LaserCBBE is 94.09% and the quality is 85.63%.

[24] For periods identified as cloudy by both retrievals, LaserCBBE minus RadarCBH differences greater than 2 km are mainly for RadarCBH less than 3 km (37 cases) or above 8 km (18 cases). For the lower heights, the differences are mainly caused by the presence of clutter, as out of the 37 cases, 29 have clutter-only flags at radar minimum CBH for more than 20% of the observational period. For these cases, the radar data processing algorithm may have mistaken some clutter particles for hydrometeors. Another possibility is that the radar detects a light drizzle not strong enough to affect the lidar returns and assigns the cloud base close to the surface. For the differences above 8 km, the radar processing most likely failed to fully detect a high thin cirrus and detected either a lower-level broken cloud with a fraction much smaller than the thin cloud above, the lowest level in the cloud or below-cloud precipitation. The difference between LaserCBBE and RadarCBH is less than -2 km for 86 soundings, but this number is reduced to 27 cases when LaserCBBE is compared with the radar minimum CBH. These disagreements are caused either by clutter areas that mask clouds, causing the radar to assign CBH to the next cloud layer, or by some thin layers detected by the lidar/ceilometer combination that are missed by the radar, again causing RadarCBH to refer to the next layer above. When LaserCBBE and RadarCBH are within 2 km of each other, the average of their differences is 0.156 ± 0.423 km with a correlation of 0.99. This difference is less than the predicted error in satellite retrievals (e.g., 1 km for MISR stereo heights [*Muller et al.*, 2002]), less than the vertical resolution of large-scale models and includes cases that could be discarded if more quality checks were performed on the radar-derived data. If we remove all cloudy cases when the amount of clutter at the level of radar minimum CBH exceeds 50% over the sounding time period, 1533 cases remain with an average difference of -0.065 ± 1.507 km and a correlation of 0.93. This result shows that the presence of clutter near cloud base tends to lower RadarCBH relative to LaserCBBE. Overall, these findings are consistent with earlier findings [e.g., *Clothiaux et al.*, 2000; *Wang and Sassen*, 2002] that, relative to even the most sensitive MMCRs, lidar/ceilometer pairs are more effective at detecting optically thin clouds whether they be cirrus or broken fair-weather cumulus.

4.2. LaserCBBE Versus CE9680CBH and CE9660CBH

[25] Of the 80 CBHs in CE9680CBH and not in LaserCBBE (Table 1, column 4), 56 cases have no RadarCBH and 8 of the 56 cases have no 3 hours LaserCBBE retrieval either. For five of these eight cases, the CE9680 approach predicts single-level clouds, while the remaining three cases are most likely moist layers. Out of the 56 cases, 31 have 3 hours LaserCBBE heights close to the CE9680CBH estimate (within 2 km), 2 cases are single-level clouds and the remaining 15 have CE9680CBH above 10 km. We suspect that the 15 cases with CE9680CBH greater than 10 km are in fact cloudless moist layers. However, we cannot discard the possibility that CE9680CBH correctly identifies clouds far from the site that do not extend over the site. The remaining 24 cases with radar detections, but no LaserCBBE, show base heights above 5 km, implying that the lidar was most likely not operational during these periods orfailed to detect high thin cloud during the daylight hours.

[26] Of the 669 CBHs in LaserCBBE not detected by CE9680CBH, 479 are detected by CE9660CBH (Table 1, column 5) while 595 are detected by CE9620CBH. In comparisons of data from fixed ground-based sensors with radiosonde-derived information, broken cloud situations will always be problematic as the two instruments are sampling different volumes of the atmosphere. For example, if we remove all cases for which the LaserCBBE cloud fraction is less than 0.2, the number of cases in LaserCBBE and not in CE9680CBH drops to 375 while for CE9660CBH the number of missed clouds drops from 190 to 102. Considering CE9620CBH, which takes into account low-clouds amounts, the number of missed cloud

Figure 1. (opposite) Histograms of frequency of cloud base and top heights occurrence as a function of cloud base or top height, respectively, for each of the seven comparisons, when both instruments detect a cloud and when one of them does not. Row a, LaserCBBE versus RadarCBH; row b, LaserCBBE versus CE9680CBH and CE9660CBH in row c; row d, LaserCBBE versus WR95CBH; row e, RadarCBH versus CE9680CBH and CE9660CBH in row f; row g, RadarCBH versus WR95CBH; row h, RadarCTH versus CE9680CTH and CE9660CTH in row i; row j, RadarCTH versus WR95CTH.

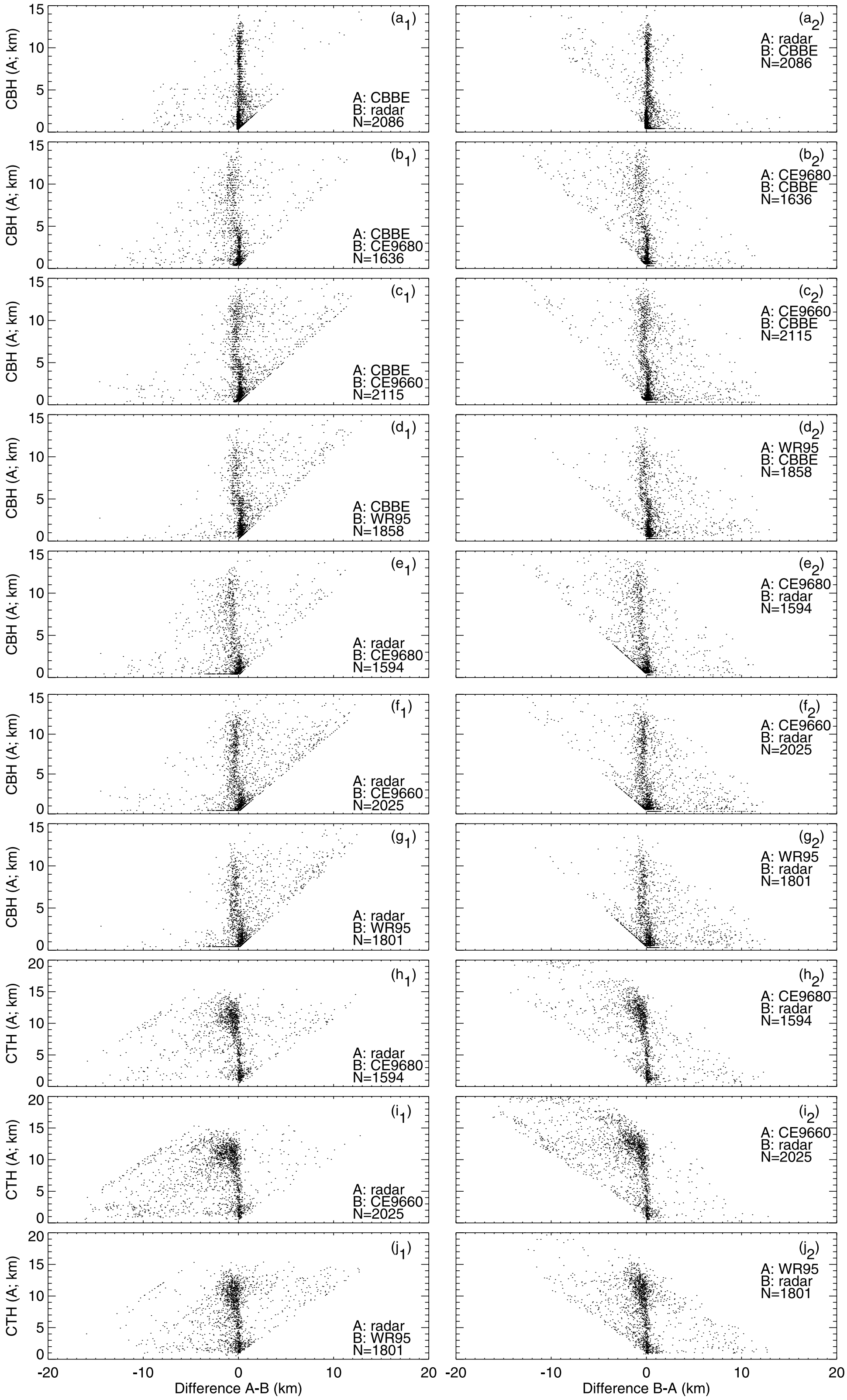

Figure 2. For all seven comparisons, cloud base height or cloud top height as a function of the difference in CBH or CTH. The repartition per row follows the same convention as in Figure 1.

cases is only 25, down from 74 cases for all LaserCBBE. These results illustrate that overall cloud detection by the CE96 technique is sensitive to the choice of the threshold on humidity.

[27] For CE9680 the detection efficiency is 95.34% higher than for the radar, meaning that this method does not overdetect clouds as much. However, the quality is only 68.6%, which means that clouds are missed more often. These results indicate that moist layers mistaken for clouds are not so much of a problem for this method, but the choice of threshold on relative humidity and scattered cloud conditions do result in missed detections. As we would expect, CE9660 with its lower relative humidity threshold is of better quality but lower efficiency.

[28] When both LaserCBBE and CE9680CBH indicate cloud, there are 180 cases with a difference less than −2 km, of which 66 cases are for CE9680 single-level clouds, and there are 75 cases with a difference greater than 2 km, of which 49 cases are for CE9680 single-level clouds. If all CE9680 single-level clouds are removed, 1076 cloudy cases remain in common between the two retrievals. The average difference becomes 0.616 ± 1.998 km with a correlation of 0.85. Considering CE9660CBH, only 76 cases have a difference between LaserCBBE and CE9660CBH that is less than −2 km and 58 of these 76 cases are for CE9660 single-level clouds. However, relative to CE9680CBH, there are many more samples with the LaserCBBE minus CE9660CBH difference exceeding 2 km. Moreover, considering only CE9660CBH single-level cloud cases leads to 138 cases when LaserCBBE is more than 2 km above CE9660CBH.

[29] We next tested a hybrid CE96 approach, called CE96HYCBH, which uses CE9680CBH below 3 km of altitude and CE9660CBH above it. This approach allows us to relax the threshold on dew-point depression for high clouds, but avoids spurious detections of clouds at lower altitudes. Of the 2115 cloudy samples, 1816 cases have a height difference between LaserCBBE and CE96HYCBH within 2 km (Table 1, column 6). For these samples, the average difference is −0.044 ± 0.559 km with a correlation coefficient of 0.99. While the CE9680CBH method tends to overestimate CBH for low clouds, the CE9660CBH tends to underestimate CBH at all heights. The hybrid method tends to underestimate CBH for clouds above 3 km and overestimate CBH below 3 km, but the number of cases which are at least 2 km above or below LaserCBBE is much smaller than when using either CE9680CBH or CE9660CBH. Although the standard deviation is larger when comparing LaserCBBE and CE96HYCBH than for the RadarCBH and CE96HYCBH comparisons, the CBHs are within 100 m of each other and the average difference is actually smaller for CE96HYCBH.

4.3. LaserCBBE Versus WR95CBH

[30] Of the 159 CBHs in WR95CBH and not in LaserCBBE (Table 1, column 7), 123 cases have no radar cloud detections and 14 of these 123 cases have no samples in 3 hours LaserCBBE. For these 123 cases, the WR95 approach has identified a moist cloudless layer as a cloud layer. For the 36 cases where LaserCBBE does not detect a cloud while both RadarCBH and WR95CBH do, RadarCBH is greater than 5 km in 34 cases, suggesting that the lidar may have failed for these retrievals and limited the detection range to 5 km. The last two cases show a large amount of clutter that may be mistaken for a cloud by the RadarCBH retrieval, whereas WR95CBH may refer to a moist cloudless layer. There are 446 CBH cases in LaserCBBE and not in WR95CBH. For 127 of these 446 cases, there is no radar CBH detection and only 19 of these 127 cases have a LaserCBBE cloud fraction greater than 0.5. These 19 cases display, in general, a high LaserCBBE with relative humidity at LaserCBBE in the range of 40–80%. For one case, although the relative humidity is large enough for WR95 to detect a cloud, the level has been eliminated when reducing the profile and for two cases the relative humidity is less than 10%. The remaining 319 cases with LaserCBBE and RadarCBH retrievals and no WR95CBH detection show a cloud fraction less than 0.5 in 122 cases. This suggests that the radiosonde may be traveling between clouds. For the remaining 197 cases, clouds are detected above 5 km in 128 cases and may be either too dry for the WR95CBH retrieval to detect them or the radiosonde may have drifted away from these clouds. For the remaining 69 cases, 38 were eliminated because the lowest layer had a top below 0.827 km and 31 had a relative humidity below 84%, being too dry to be detected by WR95CBH. The detection efficiency is less than for CE9680, but higher than for CE9660, due to detection of moist cloudless layers. The detection quality is higher than for CE9680, suggesting that the choice of relative humidity threshold is more adequate.

[31] There are 230 cases with a difference greater than 2 km, 60% of which have WR95CBH below 3 km. Using a more restrictive pair of thresholds on relative humidity (i.e., 90–93% as proposed by *Wang et al.* [1999]), about 110 of the 230 cases are removed, most of them due to eliminating spurious low-cloud detections when moist layers are present near the surface. We also found that when the difference is greater than 2 km and the radiosonde detects more than one layer, LaserCBBE tends to be close to the base of the WR95 layer above the first one. However, 65 cases have LaserCBBE above the base of the highest layer detected by WR95, which is around 10 km for these cases.

[32] When the difference between LaserCBBE and WR95CBH is less than −2 km (50 cases), LaserCBBE is mainly below 3 km. For 19 of these cases, the lowest layer detected by WR95 had a top below 0.827 km and was eliminated as a cloud layer, even though LaserCBBE was also below 0.827 km. For the remaining 31 cases, one of which was eliminated when the number of profile levels was reduced, the relative humidity at LaserCBBE is less than the 84–87% required for WR95 cloud identification.

[33] When all cases with a WR95 layer thinner than 200 m are eliminated, 1769 of the 1858 cloudy cases remain with an average difference of 0.634 ± 2.099 km and a correlation coefficient of 0.80. There are now 243 cases with height differences that exceed 2 km and for the 1526 cases with differences less then 2 km the average difference is now 0.184 ± 0.558 km with a correlation coefficient of 0.99.

[34] In summary, WR95 tends to underestimate CBH because of its tendency to classify moist cloudless layers as cloud containing layers. When this happens, LaserCBBE is often close to the base of a second WR95 cloud layer above the spurious one. For about 165 of the 1858 cases,

WR95 infers a low cloud not contained in LaserCBBE and fails to detect high clouds contained in LaserCBBE that are above the spurious cloud detections. Inspection of the WR95 results indicates that the method would perform better if the relative humidity thresholds were larger at low altitudes and smaller at high altitudes.

4.4. RadarCTH Versus CE9680CTH and CE9660CTH

[35] There are 392 cases with a RadarCTH minus CE9680CTH difference larger than 2 km (Table 1, column 10), with 107 cases having CTH differences greater than 2 km and 285 cases having CTH differences less than −2 km. Of the 107 height differences greater than 2 km, only 36 have a difference greater than 2 km in CE9660CTH (Table 1, column 11), implying that the choice of threshold for relative humidity has a large impact on CTH. For 18 of the 36 cases where the relative humidity threshold was not a factor, there were problems with the radiosonde profiles, which limit the range of detection for CE96, while 12 cases had CE9680CTH at the top of the radar layer just below the uppermost radar layer, presumably because of the low value of humidity in the highest layer. For the remaining 6 of 36 cases, 2 cases most likely had radar clutter incorrectly flagged as cloud and the last 4 cases either had erroneous radar detections or the CE96 approach failed due to measurement problems or limits in sensitivity.

[36] There are 285 cases for which RadarCTH minus CE9680CTH is less than −2 km, of which 91 cases are due to CE9680 single-level clouds. Of the 194 CE9680 multilevel clouds, 72 of them have differences between radar maximum CTH and CE9680CTH that are less than 2 km and 25 of them have differences between RadarCTH and WR95CTH that are also less than 2 km. For the remaining 97 cases, there is no correlation between the difference and the total vertical extent of the clouds retrieved from radar, the vertical extent of the highest layer detected by the radar, the wind speed at both RadarCTH and CE9680CTH or the distance between the radiosonde launch point and horizontal location when the radiosonde reached RadarCTH. As these 97 cloud cases have CE9680CTH greater than 7 km, one possible explanation is that the radar beam has been attenuated by one or more lower-level clouds and does not have sufficient sensitivity to detect the top of the highest-cloud layer. A second explanation is that the layer detected by the radiosonde is only a moist layer with no cloudiness. A final possibility is that these cases are for broken clouds and the clouds inferred from the radiosonde measurements do not extend over the radar site. Since the range of the radar is approximately 15 km and the quality of radiosonde measurements declines at low temperatures, we eliminated from the study all CE96 and WR95 cloud layers above 15 km. Such high-altitude cloud layers occurred in 114 of the CE9680CTH cases.

[37] Removing the 473 CE9680CTH single-level cloud cases from the pool of cases where both retrievals reported cloud leads to 1121 cases with an average difference of −0.944 ± 2.884 km with a correlation coefficient of 0.80. If we use the radar maximum CTH over the duration of the sounding time period in the comparisons with CE9680CTH, we arrive at an average difference of 0.180 ± 3.499 km with a correlation coefficient of 0.70. While the radar CTHs are now higher on average, the number of outliers has increased to 233 cases with differences greater than 2 km and 178 cases with differences less than −2 km. For those CTHs within 2 km of each other, the average difference is 0.162 ± 0.745 km with a correlation coefficient of 0.99. Comparing RadarCTH to CE9660CTH the average height difference is −2.419 ± 3.677 km with a correlation coefficient of 0.67. Since the CE96HY approach uses the CE9660 thresholds for high cloud, most CTH samples in CE96HYCTH will also be significantly higher than the corresponding top in RadarCTH (Table 1, column 12).

4.5. RadarCTH Versus WR95CTH

[38] For the 159 cases when RadarCTH minus WR95CTH is greater than 2 km, WR95CTH is within the top layer detected by the radar for 48 cases, is close to the radar CTH of the layer below the highest one for 54 cases and is significantly below the top of the second highest-cloud layer in 57 cases (Table 1, column 13). Of these 159 cases, WR95CTH is below the base of the lowest layer detected by the radar in 66 cases. For 20 of these 66 cases, the radar cloud fraction at cloud base is less than 0.1. Many of these differences result from the radar and radiosonde sampling different atmospheric volumes, especially for regions above 7 km, while the presence of clutter in the radar returns tends to mask clouds that are identified by WR95, leading to WR95 CTHs below the base of the lowest cloud detected by the radar. For other cases, the cloud layer detected by the radar is simply too dry to be detected by the radiosonde.

[39] Of the 269 cases where RadarCTH minus WR95CTH is less than −2 km, 46 cases have WR95CTH greater than 15 km, which we neglect, and 142 cases have a height difference between the maximum radar CTH and WR95CTH that is also less than −2 km. For the remaining 108 cases, 91 of them have RadarCTH close to the top of the second highest WR95 cloud layer, while only 5 cases have maximum radar CTHs below the base of the lowest layer detected by WR95.

[40] The correlations between the difference in radar and WR95 CTH and the geometric thickness of the top cloud layer and the total cloud vertical extent retrieved from the radar are negative. Moreover, the highest correlation coefficient is obtained for those cases where the radar CTH is within the WR95 top cloud layer. While these results are not highly significant, they do suggest that there could be some attenuation of the radar beam as clouds thicken in the vertical column above the radar. However, the response lag time of the radiosonde humidity sensor increases with cloud height, potentially leading to retrieved CTHs that will be biased high, even up to 19 km of altitude. At this stage we cannot determine which, if either, of these two measurement errors are significant and the situation is further complicated by the two instruments sampling different volumes of the atmosphere.

5. Summary and Conclusions

[41] We found that, on average, laser-derived CBHs tended to be 0.018 ± 1.559 km higher than radar-derived CBHs. There are several possible reasons for this difference, including clutter near the surface that makes identifying cloud contributions to the radar returns difficult, the presence of small particles near cloud base that the radar fails to detect, false positive cloud detections by the radar below

cloud base, and precipitation and virga below cloud base that produce significant radar returns and may prevent an accurate laser retrieval of the CBH. While the lidar can detect clouds up to 16 km at the ARM SGP site, the ceilometer is limited to a range of 5 km AGL. So when the lidar was not functioning properly, laser-derived CBHs were limited to below 5 km and height estimates for high clouds were not available.

[42] In comparisons of active sensor (i.e., laser-derived) and radiosonde-derived CBHs, we found height differences of -0.475 ± 2.303 km with the CE96 algorithm and height differences of 0.698 ± 2.240 km with the WR95 algorithm. When using the 80–100% thresholds on cloud amount in the CE96 algorithm, we found that the algorithm failed to detect the base of low-level clouds, pushing CBH up into the cloud layer, and sometimes missing the lowest cloud layer altogether. Using the 60–100% thresholds on cloud amount in the CE96 algorithm reduced these problems, but classified some moist, cloudless layers as actual cloud layers. In both approaches, the algorithm produced several single-level cloud layers when none existed, and we found that we could not eliminate these layers while keeping those that actually corresponded to actual cloud layers. We tested a hybrid CE96 method that used the 80–100% thresholds below 3 km and the 60–100% thresholds above 3 km, obtaining an average height difference of -0.054 ± 2.454 km. Overall, the hybrid method yields better agreement with the lidar/ceilometer CBHs, with fewer large discrepancies between the two and a smaller mean difference with a smaller standard deviation.

[43] While the CE96 approach tended to overestimate CBH relative to the laser-derived values, WR95 CBHs tended to be on average slightly lower. Studying the mis-detections and cases with large height differences, we concluded that the WR95 approach tended to classify moist cloudless layers as clouds, especially at lower altitudes. It also failed to detect high clouds, but this finding could result from scattered cloud situations. An inherent problem in comparisons of active sensor and radiosonde-derived cloud boundaries is that the two instruments sample different volumes of the atmosphere and there is no guarantee the instruments are sampling the same cloud types.

[44] Comparing the remote sensor (i.e., radar-derived) and radiosonde-derived CTHs, we found average height differences of -0.852 ± 3.114 km and -0.478 ± 2.944 km for CE96 and WR95, respectively. Radiosonde-derived CTHs are higher on average than those from the radar in both cases and we found that the height difference increased as CTH increased. While this difference might result from the sampling problem described above, equally likely explanations are either the cut-off in range of the radar around 15 km leading to a low bias in CTH, attenuation of the radar beam, insufficient radar sensitivity to detect cloud tops containing small particles or a slow recovery time of the radiosonde humidity sensor leading to a high bias in CTH.

[45] In summary, after removing all cases where a large difference is caused by instrumental problems and assuming laser-derived CBHs to be the most accurate, the CE96 hybrid threshold method produced the most accurate radiosonde-derived estimates of CBH for the most cases, with an average difference of -0.044 ± 0.559 km. The approach of WR95 performed almost as well with an average difference of 0.192 ± 0.564 km tending to underestimate CBH while the CE96 hybrid approach overestimated CBH. Interestingly, WR95 had the best agreement with the radar-derived CBHs because both retrievals tended to underestimate CBH relative to the laser-derived values.

[46] Overall, the radiosonde-derived CTH retrievals were consistent with each other (Table 1, columns 14 and 15). Relative to the CBH comparisons, the CTH comparisons were not as good, especially for high clouds above 10 km, with an average difference of -0.349 ± 0.745 km for CE9680CTH and -0.348 ± 0.729 km for WR95CTH. These differences are slightly more than the difference with satellite retrievals of between 0.150 and 0.300 km found by *Wang et al.* [1999] for marine stratiform (i.e., low) clouds. At this stage, without other data sources, we are not able to definitively identify the source of the large differences in the CTH retrievals. One possibility is that the radiosondes used at the SGP site (i.e., Vaisala RS80s) have a dry bias and response lag in their humidity sensor [*Miloshevich et al.*, 2002; *Wang et al.*, 2002], which affects cloud boundary assignments at high altitudes by biasing them high. Another possibility is the lack of sufficient radar sensitivity to detect the small particles at cloud top. Coincident satellite data would help in identifying scattered cloud conditions and might also aid in identifying gross errors in the ground-based retrievals. However, in order to use the ground-based data to validate satellite retrievals we must keep these two data sets independent. Other sources of in situ data, such as from aircraft, would be helpful to identify which problems are occurring on a case-by-case basis. We are continuing this study over the ARM SGP site and plan to extend it to include other sites, such as the ARM North Slope of Alaska and Tropical Western Pacific sites and Chilbolton, UK, while expanding the scope of comparisons to include satellite-derived cloud boundaries in addition to the ground-based retrievals.

[47] **Acknowledgments.** This research was supported at University College London by the European Commission under contracts ENV4-CT97-0399 (CLOUDMAP) and EVG1-CT-2000-00033 (CLOUDMAP2). E.E.C. was supported by the Office of Biological and Environmental Research of the U.S. Department of Energy (under grant DE-FG02-90ER61071) as part of the Atmospheric Radiation Measurement (ARM) Program. Data were obtained from the Atmospheric Radiation Measurement (ARM) Program sponsored by the U.S. Department of Energy, Office of Biological and Environmental Research, Environmental Sciences Division. The authors would like to thank Oleg Alduchov for his invaluable help in analyzing the radiosonde profiles.

References

Alduchov, O. A., and E. E. Eskridge, Improved magnus' form approximation of saturation vapor pressure, *J. Appl. Meteorol.*, *35*, 601–609, 1996.

Arabey, E. N., Radiosonde data as means for revealing cloud layers, *Meteorol. Gidrol.*, *6*, 32–37, 1975.

Baum, B. A., T. Uttal, M. Poellot, T. P. Ackerman, J. M. Alavarez, J. Intrieri, D. O'C. Starr, J. Titlow, V. Tovinkere, and E. Clothiaux, Satellite remote sensing of multiple cloud layers, *J. Atmos. Sci.*, *52*, 4210–4230, 1995.

Chernykh, I. V., Averages of relative humidity at the cloud base level, in *WMO Rep. 28*, *WMO/TD 942*, pp. 2.7–2.8, 1999.

Chernykh, I. V., and O. A. Alduchov, Comparison of cloud layers detecting by different methods, Proceedings of the Fifth International Cloud Modeling Workshop, Aug. 2000, Colo., USA, 2000.

Chernykh, I. V., and R. E. Eskridge, Determination of cloud amount and level from radiosonde soundings, *J. Appl. Meteorol.*, *35*, 1362–1369, 1996.

Chernykh, I. V., O. A. Alduchov, and R. E. Eskridge, Trends in low and high cloud boundaries and errors in height determination of cloud boundaries, *Bull. Am. Meteorol. Soc.*, *82*, 1941–1947, 2001.

Clothiaux, E. E., G. G. Mace, T. P. Ackerman, T. J. Kane, J. D. Spinhirne, and V. S. Scott, An automated algorithm for detection of hydrometeor returns in micro pulse lidar data, *J. Atmos. Oceanic Technol.*, *15*, 1035–1042, 1998.

Clothiaux, E. E., T. P. Ackerman, G. C. Mace, K. P. Moran, R. T. Marchand, M. A. Miller, and B. E. Martner, Objective determination of cloud heights and radar reflectivities using a combination of active remote sensors at the ARM CART sites, *J. Appl. Meteorol.*, *39*, 645–665, 2000.

Curry, J. A., et al., FIRE Arctic clouds experiment, *Bull. Am. Meterol. Soc.*, *81*, 5–19, 2000.

Dong, X., P. Minnis, T. P. Ackerman, E. E. Clothiaux, G. C. Mace, C. N. Long, and J. C. Liljegren, A 25-month database of stratus cloud properties generated from ground-based measurements at the Atmospheric Radiation Measurement Southern Great Plains site, *J. Geophys. Res.*, *105*, 4529–4537, 2000.

Han, D., and R. G. Ellingson, An experimental technique for testing the validity of cumulus cloud parameterisations for longwave radiation calculations, *J. Appl. Meteorol.*, *39*, 1147–1159, 2000.

Mace, G. G., T. P. Ackerman, P. Minnis, and D. F. Young, Cirrus layer microphysical properties derived from surface-based millimeter radar and infrared interferometer data, *J. Geophys. Res.*, *103*, 23,207–23,216, 1998.

Marchand, R. T., T. P. Ackerman, M. D. King, C. Moroney, R. Davies, J.-P. A. L. Muller, and H. Gerber, Multiangle observations of arctic clouds from FIRE ACE: June 3, 1998, case study, *J. Geophys. Res.*, *106*, 15,201–15,214, 2001.

Menzel, W. P., Cloud tracking with satellite imagery: From the pioneering work of Ted Fujita to the present, *Bull. Am. Meteorol. Soc.*, *82*, 33–47, 2001.

Miloshevich, L. M., H. Vomel, A. Paukkunen, A. J. Heymsfield, and S. J. Oltmans, Characterization and correction of relative humidity measurements from vaisala RS80-A radiosondes at cold temperatures, *J. Atmos. Oceanic Technol.*, *18*, 135–156, 2002.

Muller, J.-P., A. Mandanayake, C. Moroney, R. Davies, D. J. Diner, and S. Paradise, MISR stereoscopic image matchers: Techniques and results, *IEEE Trans. Geosci. Remote Sens.*, *40*, 1547–1559, 2002.

Office of the Federal Coordinator for Meteorology, *Federal Meteorological Handbook,* vol. 3, *Rawinsonde and Pibal Observations, FCM-H3-1997*, Silver Spring, Md., 1997.

Ou, S. C., K. N. Liou, and T. R. Caudill, Remote sensing of multilayer cirrus cloud systems using AVHRR data collected during fire-II-IFO, *J. Appl. Meteorol.*, *37*, 241–254, 1998.

Poore, K. D., J. Wang, and W. B. Rossow, Cloud layer thicknesses from a combination of surface and upper-air observations, *J. Clim.*, *8*, 550–568, 1995.

Schmetz, J., K. Holmlund, J. Hoffman, B. Strauss, B. Mason, V. Gaertner, A. Koch, and L. Vandeberg, Operational cloud-motion winds from METEOSAT infrared images, *J. Appl. Meteorol.*, *32*, 1206–1225, 1993.

Slingo, J. M., A cloud parametrization scheme derived from GATE data for use with a numerical model, *Q. J. R. Meteorol. Soc.*, *106*, 747–770, 1980.

Smith, W. L., and C. M. Platt, Comparison of satellite deduced cloud heights with indications from radiosonde and ground based laser measurements, *J. Appl. Meteorol.*, *17*, 1796–1802, 1978.

Trishchenko, A. P., Z. Li, F.-L. Chang, and H. Barker, Cloud optical depths and TOA fluxes: Comparison between satellite and surface retrievals from multiple platforms, *Geophys. Res. Lett.*, *28*(6), 979–982, 2001.

Wang, J., and W. B. Rossow, Determination of cloud vertical structure from upper-air observations, *J. Appl. Meteorol.*, *34*, 2243–2258, 1995.

Wang, J., W. B. Rossow, T. Uttal, and M. Rozendaal, Variability of cloud vertical structure during ASTEX observed from a combination of rawinsonde, radar, ceilometer and satellite, *Mon. Weather Rev.*, *127*, 2484–2502, 1999.

Wang, J., W. B. Rossow, and Y. Zhang, Cloud vertical structure and its variations from a 20 yr global rawinsonde dataset, *J. Clim.*, *13*, 3041–3056, 2000.

Wang, J. H., H. L. Cole, D. J. Carlson, E. R. Miller, K. Beierle, A. Paukkunen, and T. K. Laine, Corrections of humidity measurement errors from the Vaisala RS80 radiosonde-application to TOGA COARE data, *J. Atmos. Oceanic Technol.*, *9*, 981–1002, 2002.

Wang, Z., and K. Sassen, Cirrus cloud microphysical property retrieval using lidar and radar measurements, part II, Midlatitude cirrus microphysical and radiative properties, *J. Atmos. Sci.*, *59*, 2291–2302, 2002.

E. E. Clothiaux, Pennsylvania State University, University Park, PA 16802, USA.

J.-P. Muller and C. M. Naud, Geomagnetic Engineering, University College, Gower Street, London, WC1E 6BT, UK. (cnaud@ge.ucl.ac.uk)